Biosensors and Bioelectronics 141 (2019) 111472

Contents lists available at ScienceDirect

Biosensors and Bioelectronics

journal homepage: www.elsevier.com/locate/bios

High-resolution temporally resolved chemiluminescence based on double-layered 3D microfluidic paper-based device for multiplexed analysis

Fang Li[a,*], Jiachang Liu[a], Lei Guo[a], Jihang Wang[a], Kaiqi Zhang[a], Jianbo He[a], Hua Cui[b]

[a] Anhui Province Key Laboratory of Advanced Catalytic Materials and Reaction Engineering, School of Chemistry and Chemical Engineering, Hefei University of Technology, Hefei, Anhui, 230009, People's Republic of China

[b] CAS Key Laboratory of Soft Matter Chemistry, Collaborative Innovation Center of Chemistry for Energy Materials, Department of Chemistry, University of Science and Technology of China, Hefei, Anhui, 230026, PR China

ARTICLE INFO

Keywords:
μPAD
Temporally resolved chemiluminescence
High resolution
Multiplexed analysis

ABSTRACT

In this work, a double-layered three-dimensional (3D) microfluidic paper-based analytical device (μPAD) with high resolution temporally resolved chemiluminescence (CL) emissions were designed for multiplexed CL analysis. The temporally resolved CL emissions were obtained by virtue of the 3D branched microfluidic channel design, which create time delays for luminol transported from one detection zone to another. The peak intensity and peak shape of the temporally resolved CL emissions were quite stable and base-line separated with resolution as high as 21.2–24.4. Then, the fabricated μPAD was applied to multiplexed determination of glucose, lactate, cholesterol, and choline as model analytes. The sample was added to four detection zone modified with CL catalyst cobalt ion and different oxidase by virtue of chitosan. When luminol flowed to μPAD, four temporally resolved CL peaks were successively generated from the cobalt ion catalyzed CL reactions between luminol and generated H_2O_2 from the specific enzymatic reactions between the oxidase and the analytes. The generated four CL emission peaks in the CL kinetic curve increased in proportion to the concentrations of glucose, lactate, cholesterol, and choline, respectively. Finally, four linear calibration curves were obtained for the detection of glucose (0.01–1.0 mmol/L), lactate (0.02–5.0 mmol/L), cholesterol (0.01–0.4 mmol/L), and choline (0.001–1.0 mmol/L). The detection limits were as low as 8 μmol/L, 15 μmol/L, 6 μmol/L, and 0.07 μmol/L for glucose, lactate, choline, and cholesterol detection, respectively. The present work provides a new strategy for the fabrication of simple and sensitive 3D μPAD with high resolution temporally resolved CL emissions for multiplexed CL analysis, which holds great application potential for point-of-care diagnosis.

1. Introduction

The increase of aging population and growth of health concerns promoted the development of novel analytical methods to detect biomarkers for point-of-care testing (POCT) (Ding et al., 2019; Syedmoradi et al., 2017). Multiplexed analysis, which could not only save time, reagent, cost and labor, but also determine simultaneously multiple analytes in a single sample, have attracted increasing attentions in POCT. Microfluidic paper-based analytical devices (μPADs) combined the advantages of test papers and the capability of lab-on-chip devices were developed in 2007 by Whitesides' group (Martinez et al., 2007). The surface of μPADs were patterned and constructed into desired hydrophilic microchannels and hydrophobic barrier by virtue of a variety of methods (Dungchai et al., 2009; Jang and Song, 2015; Wang et al., 2012; Yamada et al., 2015), to enable multiple distribution of solutions on a single microfluidic device. Integrating of sample collection, pretreatment, directional transport, specific reaction, and detection together on one minimized device, μPADs are very attractive and hold great potential for multiplexed analysis (Xia et al., 2016). So far, colorimetric (Lopez-Ruiz et al., 2014; Morbioli et al., 2017b), fluorescent (Liang et al. 2016, 2017), and electrochemical (Chaiyo et al., 2016; Rattanarat et al., 2014) detection methods combined with visual perception, spectral analysis and potential discrimination, respectively, are the primary analytical technologies integrated with μPADs for multiplexed analysis. The development of novel simple and sensitive μPADs is still highly desired.

Chemiluminescence (CL) is an attractive detection method due to its simplicity, low cost, high sensitivity, wide calibration range, low background, and simple instrumentation with no requirements of excitation source or optical filters. The usefulness of CL makes it an attractive detection method for μPADs. Generally, the CL signals were generated by mixing the CL reagent with the oxidizing reagent in the

* Corresponding author.
E-mail address: lifang@hfut.edu.cn (F. Li).

https://doi.org/10.1016/j.bios.2019.111472
Received 1 April 2019; Received in revised form 18 June 2019; Accepted 23 June 2019
Available online 25 June 2019
0956-5663/

presence of horseradish peroxidase or some metal ions as catalyst. Usually, only one CL emission peak was observed in the CL kinetic curve. Thus, the traditional μPADs integrated with CL detection were difficult to be used for multiplexed analysis. Later on, μPADs with temporal resolution were designed for multiplexed CL analysis. For example, Yu's group first reported a μPAD based CL biosensor for the simultaneous detection of glucose and uric acid by designing two microchannels with different distance for glucose and uric acid sample transport, respectively (Yu et al., 2011). However, the reported μPAD based CL biosensor still need some improvements. For example, the obtained two CL emission peaks used for the quantification of glucose and uric acid were overlapped seriously. Furthermore, only two kinds of analytes were determined and the detection limits were high. Recently, Liu's group reported a μPAD based CL immunodevice for the simultaneous determination of three kinds of antigens by using sugar as barrier to obtain solution migration delay from one microchannel to another (Chu et al., 2017). However, the use of dissolvable sugar as barrier to obtain migration time delay suffered from the disadvantages that the sucrose might be washed off from the microchannels and cause instability and cross contamination of the microchannels. Furthermore, the reported two approaches were both traditional two-dimensional (2D) μPAD. Recently, the design and fabrication of three-dimensional (3D) μPADs have attract lots of interests (Lewis et al., 2012; Morbioli et al., 2017a). 3D μPAD allow solution to flow both laterally and vertically, permit individually layer treatment, make parallel and multiplexed analysis possible, and could effectively eliminating cross contamination. For example, Yu's group proposed a 3D origami-based μPAD for multiplexed CL analysis of four tumor markers (Ge et al., 2012). However, the 3D μPAD encountered a problem that the CL peak heights of the four temporally resolved CL emissions decreased successively. The relative standard deviation (RSD) of the four CL peak heights for the determination of the same analyte was greater than 23.2%. In addition, serious peak broadening phenomenon was encountered with the CL peak width at base increased from 5.5 s to 23 s. As a result, the resolution of this temporally resolved CL biosensor still need improvement.

In the present work, a novel double-layered 3D μPAD with high-resolution temporally resolved CL emissions was designed without the use of any barrier reagent. Solution migration time delays from one detection zone to another was obtained by virtue of branched 3D microfluidic channels. CL catalyst cobalt ion and different oxidases were pre-modified on the detection zones by virtue of chitosan. H_2O_2 were generated from the specific enzymatic reactions between the oxidase and the analytes at the detection zones. When luminol flowed through the 3D μPAD, temporally resolved CL emissions were generated from the cobalt ion catalyzed CL reactions between luminol and generated H_2O_2. The temporally resolved CL emissions occurred from different detection zones could be used for multiplexed CL analysis. Thus, a simple CL biosensor for the sensitive, selective and simultaneous determination of glucose, lactate, cholesterol, and choline were fabricated based on the fabricated 3D μPAD. The analytical performance of the CL biosensor, including sensitivity, selectivity and stability, was investigated. The practical applicability of the CL biosensor in serum samples was explored.

2. Experimental section

2.1. Chemicals and materials

Luminol was purchased from Tokyo Chemical Industry Co., Ltd. (Shanghai, China) and a 10 mmol/L luminol stock solution was prepared in 0.1 mol/L NaOH solution. Chitosan powder (M_v > 1000 kDa, degree of deacytylation > 90%), cobalt chloride, glucose, lactate, cholesterol, choline, and paraffin (melting points 48–50 °C) were purchased from Sinopharm Chemical Reagent Co. (Shanghai, China). Whatman chromatography paper (WCP#1, 20 cm × 20 cm), glucose oxidase, and lactate oxidase were purchased from Solarbio Biotechnology Co. Ltd. (Beijing, China). Cholesterol oxidase and choline oxidase were purchased from Sigma-Aldrich (St. Louis, USA). All other reagents were of analytical grade. Ultrapure water was used throughout.

2.2. Design and fabrication of the 3D μPAD.

Firstly, the pattern of the μPAD was designed using Auto CAD software (Autodesk Inc.). The μPAD was composed of two layers of papers, including the top auxiliary layer and the bottom CL detection layer. As shown in Fig. S1A, the top auxiliary layer of μPAD was composed of one central sampling zone, four branched microfluidic channels, and four small sampling zones (No. 1, 2, 3, 4). The diameter of central sampling zone was 10 mm, the diameter of small sampling zones was 6 mm, the width of channels was 3 mm. The length of the branched microfluidic channel was 8 mm. The deflecting angle of the branched microfluidic channels was 60°. As shown in Fig. S1B, the bottom CL detection layer of the μPAD was consisted of one central zone and four detection zones (No. 1, 2, 3, 4). The small sampling holes on the top auxiliary layer were vertical overlapped with the detection zones on the bottom layer. Thus, the solution injected to the central sampling zone on the top auxiliary layer could migrate laterally to the small sampling zones and then flow vertically downward to the corresponding detection zones on the bottom detection layer by overlapping the two layers in alignment to construct 3D μPAD, as shown in Fig. S1C.

The hydrophilic microfluidic channels and hydrophobic barrier on the two layers of the μPAD were fabricated by a simple wax-screen-printing technology according to our previous work (Wang et al., 2018). Screen stencils made by 200 mesh of nylon mesh printed with impenetrable photosensitive emulsion according to the designed μPAD patterns were produced at a local printing shop. The screen stencil was closely placed on top of the paper, and then brushed through the screen stencil with a piece of paraffin. The paraffin penetrated the pores of the screen stencil, forming wax patterns on the paper. Then, the wax-screen-printed papers were heated in an oven set at 100 °C for 30 s, allowing the wax to melt and penetrate inside the paper structure, forming hydrophobic barriers on μPAD. The impermeable barrier on the screen stencil formed the hydrophilic microfluidic channels of μPAD. The fabricated top auxiliary layer was ready for use, while the bottom detection layer need further modification.

2.3. Modification of the detection layer of the 3D μPAD.

In this work, μPAD with four detection zones was chosen as a model analytical device for multiplexed analysis of glucose, lactate, cholesterol, and choline. For multiplexed CL analysis, the detection layer of the μPAD was modified as follows. Firstly, 2 μL of 1 mg/mL chitosan mixed with 0.5 mmol/L cobalt chloride was added to the four detection zones on the detection layer. Then, 2 μL 0.2 kU/mL glucose oxidase, 2 μL 6 U/mL lactate oxidase, 2 μL 7 mg/mL cholesterol oxidase and 2 μL 0.2 mg/mL choline oxidase dissolved in pH 7.5 phosphate buffer was added to the detection zone No. 1, 2, 3, and 4, respectively. Then, 2.0 μL sample solution containing a series of different concentrations of glucose, lactate, cholesterol, and choline were added to the four detection zones, followed by incubation at room temperature for 6 min. Finally, the detection layer and the auxiliary layer were overlapped in alignment and fixed in tight contact to form 3D μPAD for CL detection.

2.4. Multiplexed CL analysis

The CL measurements were carried on an ultraweak luminescence analyzer (MPI-A, Xi'an Remex, Xi'an, China). For CL measurement, the 3D μPAD was put on top of the photomultiplier tube. Then, 100 μL 10 mmol/L luminol solution dispersed in 0.1 mol/L NaOH was added to the central sampling zone of the 3D μPAD. The added luminol solution

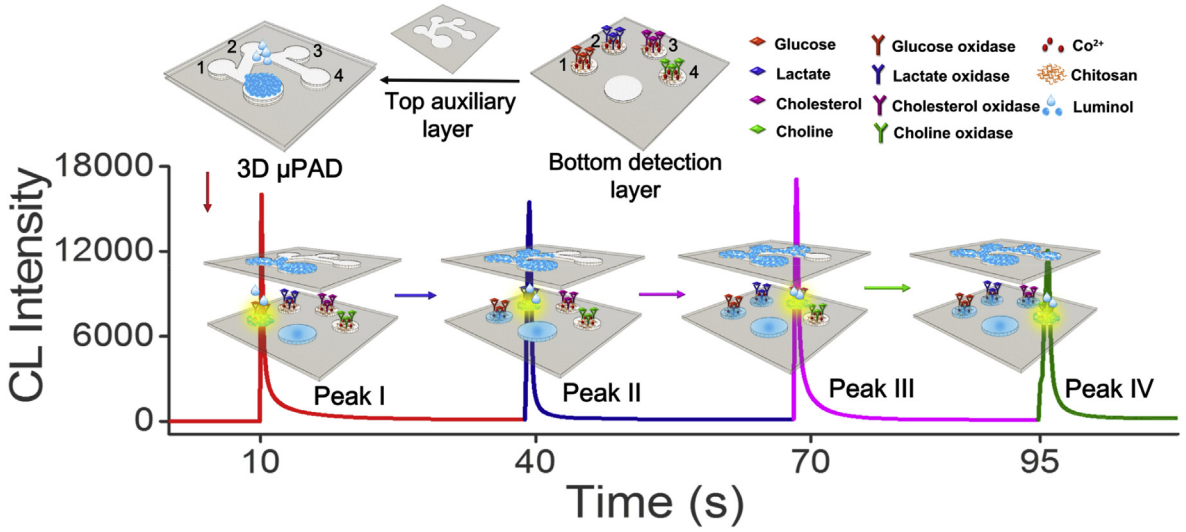

Fig. 1. Schematically illustration for fabrication of 3D μPAD for multiplexed CL analysis. Detection zone No.1: glucose detection zone, No.2: lactate detection zone, No.3: cholesterol detection zone, No.4: choline detection zone.

migrated to the four detection zones sequentially to initiate the CL reactions. Then, four temporally resolved CL emission peaks corresponded to the four CL reactions occurred at the four detection zones were recorded in the CL intensity-versus-time profile. The concentration of glucose, lactate, cholesterol, and choline could be quantified by reading the CL intensity of the four CL peaks, respectively.

3. Results and discussion

3.1. Principle for multiplexed CL analysis based on the 3D μPAD.

Small biomolecules including glucose, lactate, cholesterol, and choline were chosen as model analytes. Before multiplexed CL analysis, the feasibility of the proposed paper-based sensing strategy was verified by determination each analyte at their respective detection zone by using the bottom detection layer as sensing platform. The four detection zones were modified with chitosan, cobalt ion and different kinds of oxidases. The modified specific oxidase on the four detection zones was glucose oxidase, lactate oxidase, cholesterol oxidase, and choline oxidase for glucose, lactate, cholesterol, and choline detection, respectively. Chitosan is a biocompatible substance with high specific surface area and good film-forming ability, which could form a thin film on the porous structure of cellulose paper through electrostatic interactions and physical absorption (Rinaudo, 2006). CL catalyst cobalt ion were co-immobilized by virtue of the chelating reactions between cobalt ion and amino groups from chitosan (Guibal, 2004). The chitosan film on cellulose paper provided a good support to adsorb enzymes, and constructed a biocompatible microenvironment to maintain the reactivity of enzymes (Gabriel et al., 2016). Then, different concentration of glucose, lactate, cholesterol, and choline were added to their respective detection zones followed by incubation at room temperature for 6 min. After that, 12 μL luminol solution was directly added to each detection zone to initiate the CL reactions. As shown in Figs. S2–5, CL emissions were observed at the four detection zones and the CL intensity increased gradually with the increasing of the concentration of the corresponding analyte, respectively. It indicated that the four oxidases were successfully immobilization on the detection zones by virtue of chitosan, and the immobilized oxidases work well to generate H_2O_2 for CL reaction. The added luminol reacted with the generated H_2O_2 to produce strong CL emissions with co-immobilized cobalt ion as catalyst. The more analyte existed in the detection zones, the more H_2O_2 could be generated, resulting in increased CL intensity. As seen in the inserted figures in Figs. S2–5, linear relationships were obtained at each detection zone for the determination of glucose, lactate, cholesterol, and choline, respectively. Thus, the feasibility of the proposed paper-based sensing strategy was verified and the developed paper-based sensing strategy could be used to the determination of the four small biomolecules.

In order to achieve multiplexed CL analysis, μPAD with special geometry to produce time delay in the delivery of luminol to different detection zones was needed. The luminol solution was transported by virtue of the top auxiliary layer. Thus, the geometry of the top auxiliary layer was optimized. Eighteen kinds of top auxiliary layer with different geometries (as shown in Fig. S6) were tested. It was found that the stability and temporally resolved ability of the present top auxiliary layer was the best (data not shown). Then, the solution migration on the 3D μPAD composed by the optimized top auxiliary layer was further investigated. As shown in Fig. S7, after the injection of 100 μL blue dye solution (copper ammoniate complex-ion solution) to the central sampling zone of the top auxiliary layer, the blue solution driven by capillary force migrated laterally to the small sampling zone No. 1 on the top auxiliary layer immediately, and continued migrating downward to the detection zone No. 1 on the bottom detection layer in 10 s. Sequentially, another distributary of the solution flowed laterally and vertically to the detection zone No. 2 in 40 s, and then the detection zone No. 3 in 70 s, and then the detection zone No. 4 in 95 s. Thus, solution migration delays from one detection zone to another were obtained by virtue of the 3D branched microfluidic channels. The solution arrived at the detection zones detained in situ and 100 μL solution was just enough to fully fill the detection zones. The top auxiliary layer and the bottom detection layer could cling closely to each other after the diffusion of the solution from the top layer to the bottom layer due to the adhesion and cohesion forces of the liquid. The self-adhesion of the two layers could create an unimpeded 3D microfluidic channels for sample migration. It demonstrated that the microfluidic channels of the 3D μPAD were successfully fabricated and long enough time intervals were obtained for temporally resolved CL detection.

Then, the multiplexed CL analysis ability of the proposed 3D μPAD was further investigated. Fig. 1 schematically illustrated the fabrication of the 3D μPAD for multiplexed determination of the four small biomolecules. The four detection zones were modified as described previously. The sample mixtures containing glucose, lactate, cholesterol, and choline were added to the four detection zones. H_2O_2 were generated in the detection zones through the specific oxidase enzymatic reactions between the oxidases and the corresponding analyte. Then, the top auxiliary layer and the bottom detection layer were overlapped

in alignment to obtain 3D μPAD. Afterward, luminol solution was injected to the central sampling zone on the top auxiliary layer. The injected luminol solution migrated through the branched 3D microfluidic channels and arrived sequentially in the four detection zones, i.e. glucose detection zone, lactate detection zone, cholesterol detection zone and choline detection zone. After arrived in the detection zones, luminol reacted with the generated H_2O_2 with the co-immobilized cobalt ion as CL catalyst, producing strong CL emissions immediately. Since the migration times of luminol to the four detection zones were different, the CL reactions from the four detection zones occurred sequentially. The CL kinetic curve in Fig. 1 shows the typical CL response of the 3D μPAD in the presence of 1.0 mmol/L glucose, 5.0 mmol/L lactate, 0.4 mmol/L cholesterol, and 1.0 mmol/L choline. It can be seen that four steep well-separated temporally resolved CL emission peaks were generated in the CL intensity-versus-time profile in one CL detection. The CL curves of the four temporally resolved CL peaks were sharp, demonstrating that the CL reaction between luminol and generated H_2O_2 catalyzed by cobalt ion was very quick. The four CL peaks corresponded to the CL reaction from the glucose (peak I), lactate (peak II), cholesterol (peak III), and choline (peak IV) detection zone, respectively, could be used for multiplexed determination of the four small molecules.

3.2. Characteristic of the temporally resolved CL emissions based on the 3D μPAD.

Temporally resolved CL emissions for multiplexed analysis were obtained based on the developed 3D μPAD. The CL behavior of this 3D μPAD for the determination of glucose at the four detection zones simultaneously was also carried out. Then, the four detection zones were all immobilized with glucose oxidase. Fig. 2 shows the CL kinetic curve of this 3D μPAD in the presence of 0.7 mmol/L glucose. As expected, four base-line separated temporally resolved CL peaks were obtained in one CL detection and no decrease in CL intensity and no peak broadening phenomenon was observed. The CL peak height of the four CL emissions was 9 798, 9 993, 10 324, 9759 a. u., respectively, with RSD of the peak heights as small as 2.6%. The CL peak widths at base were small and steady ranging from 1.1 to 1.4 s. The time intervals between adjacent CL peaks were long and even ranging from 26 to 30 s. It indicated that the CL intensity and CL peak shape kept stable with the increase of the solution migration distance. The resolution of the temporally resolved CL emissions calculated according to chromatographic resolution were 22.1, 24.4 and 21.2 for the adjacent CL peaks. Resolution value higher than 1.5 was recognized as completely separation and indicated no interference between adjacent peaks. Thus, the four temporally resolved CL emissions in this work were completely separated and the previous CL emission has no effect on the successive one. In comparison, the resolution were calculated to be 0.8, 0.9, and 1.0 for the reported 3D μPAD with linear flow channel design, which were much smaller than the resolutions achieved in this work (Ge et al., 2012). It demonstrated that the developed 3D μPAD with branched 3D microfluidic channels exhibited rather high resolution quite suitable for multiplexed CL detection.

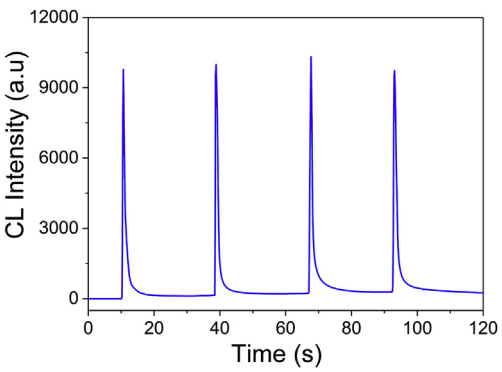

Fig. 2. CL kinetic curve of 3D μPAD for determination of 0.7 mmol/L glucose at four detection zones.

3.3. Comparison study with one-layered 2D μPAD.

In this work, double-layered 3D μPAD was designed to obtain temporally resolved CL emissions. To compare, traditional one-layered 2D μPAD was also fabricated (Fig. S8A). The pattern of the one-layered 2D μPAD was similar to the top auxiliary layer of the double-layered 3D μPAD. The four detection zones of the 2D μPAD (No. 1, 2, 3, and 4) were modified with chitosan, cobalt ion and different kinds of oxidase according to the modification procedure of the detection layer of the 3D μPAD. Then, sample solution containing 1.0 mmol/L glucose, 5.0 mmol/L lactate, 0.4 mmol/L cholesterol, and 1.0 mmol/L choline were added to the four detection zones of the 2D μPAD and incubated for 6 min. Then, luminol solution was added to the central sampling zone of the 2D μPAD. The added luminol solution migrated laterally and sequentially to the four detection zones to initiate CL reactions. As shown in Fig. S8B, four CL peaks were recorded in the CL intensity-versus-time profile with the 2D μPAD in one CL detection. However, the four CL peaks were broad and partly overlapped. In comparison, the four CL peaks obtained with the double-layered 3D μPAD were steep and base-line separated (Fig. 1). The RSDs of the CL intensities from each detection zone were calculated to be between 7.64% and 15.64% in three repeated experiments with the 2D μPAD, while the RSDs of the CL intensities were only between 3.51% and 6.54% with the double-layered 3D μPAD. Thus, the difference in CL intensities from parallel detections was much smaller with the double-layered 3D μPAD than that with the one-layered 2D μPAD. Furthermore, the CL intensities obtained with the 3D μPAD (16 026, 15 599, 17 131, 11 956 a. u., respectively) were about 1 order of magnitude higher than that obtained with the 2D μPAD (1529, 1737, 1880, 1681 a. u., respectively). Such improvements in both reproducibility and CL intensity were mainly attributed to the special vertically injecting effect of double-layered 3D μPAD for solution migrating from the top layer to the bottom layer. The luminol solution could fill into the whole detection zone rapidly through the full-contacted of the small sampling zones on the top layer and the detection zones on the bottom layer. In comparison, the laterally migration of luminol solution from the microfluidic channels to the detection zones on the one-layered 2D μPAD were slow and progressive, resulting in broadened CL peak shape and weakened CL intensities. Thus, great improvements in reproducibility, sensitivity and resolution could be obtained by using the proposed double-layered 3D μPAD than traditional one-layered 2D μPAD.

3.4. Analytical performance of 3D μPAD for multiplexed CL analysis

Before the CL analysis, the important detection conditions including the concentrations of chitosan, glucose oxidase, lactate oxidase, cholesterol oxidase, choline oxidase, and cobalt ion catalyst on the detection zones, the incubation time to generate H_2O_2, the category and pH of buffer, and concentration of luminol for CL reaction were optimized. As shown in Figs. S9–S13, the optimized concentration of chitosan, glucose oxidase, lactate oxidase, cholesterol oxidase, choline oxidase and cobalt ion was 1 mg/mL, 0.2 kU/mL, 6 U/mL, 7 mg/mL, 0.2 mg/mL and 0.5 mmol/L, respectively. The optimized incubation time was 6 min. The optimized concentration of luminol and buffer solution was 10 mmol/L luminol dispersed in 0.1 mol/L NaOH.

Under the optimal detection conditions, the analytical performance of the proposed 3D μPAD for the simultaneous determination of glucose, lactate, cholesterol, and choline was investigated. Fig. 3A shows the typical CL responses of the proposed 3D μPAD in the presence of different concentrations of glucose, lactate, cholesterol, and choline. The CL response of the proposed 3D μPAD in the absence of analytes

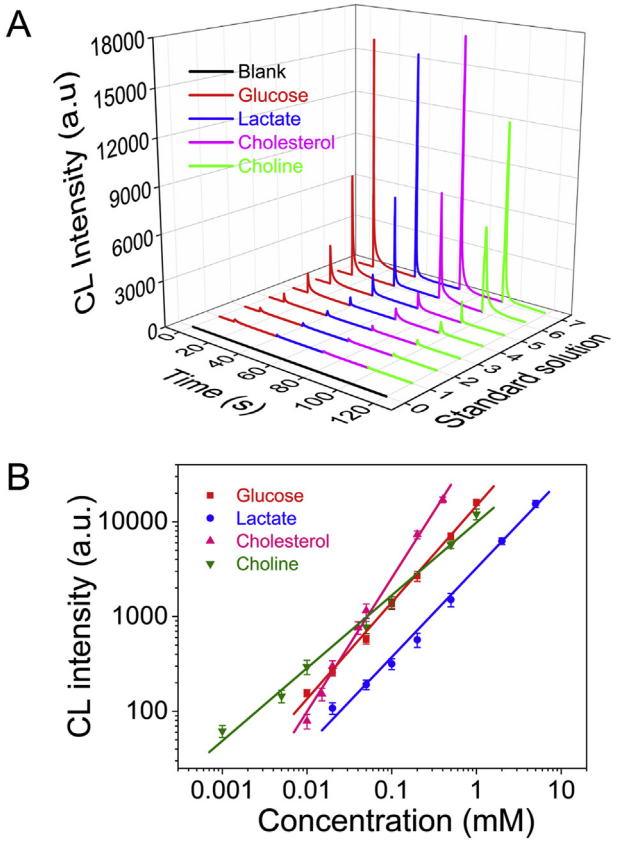

Fig. 3. (A) CL responses of 3D μPAD in the presence of different concentrations of glucose, lactate, cholesterol, and choline. The concentration of glucose, lactate, cholesterol, and choline in the standard solution No. 0: blank, No. 1: 0.01, 0.02, 0.01, 0.001 mmol/L, No. 2: 0.02, 0.05, 0.015, 0.005 mmol/L, No. 3: 0.05, 0.1, 0.02, 0.01 mmol/L, No. 4: 0.1, 0.2, 0.04, 0.05 mmol/L, No. 5: 0.2, 0.5, 0.05, 0.1 mmol/L, No. 6: 0.5, 2.0, 0.2, 0.5 mmol/L, No. 7: 1.0, 5.0, 0.4, 1.0 mmol/L, respectively. (B) Representative calibration curves for glucose, lactate, cholesterol, and choline detection based on the developed 3D μPAD.

were at base line (black line). Four steep high-resolution temporally resolved CL emission peaks were recorded in the presence of various concentrations of glucose, lactate, cholesterol, and choline. The four CL emissions were generated from the CL reactions between luminol and generated H_2O_2 catalyzed by cobalt ion. The more corresponding analyte existed in the mixture, the more H_2O_2 would be generated in the detection zone. Accordingly, the peak height of the four temporally resolved CL emissions in the CL kinetic curves increased gradually with the increasing of the concentration of glucose, lactate, cholesterol, and choline, respectively. Quantitative analysis of the four small biomolecules were realized by reading the CL intensities of the four temporally resolved CL peaks. As shown in Fig. 3B, four linear calibration curves were obtained for the simultaneous determination of glucose, lactate, cholesterol, and choline. For glucose detection, the calibration curve was $\log I = 4.17 + 1.02 \log C$, $R^2 = 0.996$, with linear range from 0.01 to 1.0 mmol/L. For lactate detection, the calibration curve was $\log I = 3.51 + 0.94 \log C$, $R^2 = 0.995$, with linear range from 0.02 to 5.0 mmol/L. For cholesterol detection, the calibration curve was $\log I = 4.81 + 1.41 \log C$, $R^2 = 0.996$, with linear range from 0.01 to 0.4 mmol/L. For choline detection, the calibration curve was $\log I = 3.99 + 0.77 \log C$, $R^2 = 0.991$, with linear range from 0.001 to 1.0 mmol/L. In the equations above, I was the CL intensity and C was the concentration of the corresponding analyte (mM). The detection limits were 8 μmol/L for glucose, 15 μmol/L for lactate, 6 μmol/L for cholesterol, and 0.7 μmol/L for choline, respectively, which were calculated from the regression equations at a signal-to-noise ratio of 3 (S/N = 3). The detection limit in this work was more than one order of magnitude lower than the previously reported μPAD based CL biosensor for glucose detection (Yu et al., 2011). Such high sensitivity was mainly ascribed to the special double-layered 3D μPAD design combined with the great catalytic effect of co-immobilization cobalt ion on the luminol-H_2O_2 CL reaction, resulting in highly enhanced CL intensity (Lin et al., 2001). Furthermore, even though CL assays have been reported for the determination of lactate (Nakamura et al., 2001), cholesterol (Mike and Cleland, 1992), and choline (Tsafack et al., 2000), as far as we known, there is still no report about μPAD based CL biosensor for lactate, cholesterol or choline detection. As shown in Table S1, the RSD were below 5.54% within a day and below 8.81% in different days for the determination of glucose (1.0 and 0.5 mmol/L), lactate (5.0 and 2.0 mmol/L), cholesterol (0.4 and 0.2 mmol/L), and choline (1.0 and 0.5 mmol/L), indicating good repeatability and reliability of the μPAD based CL biosensor.

3.5. Selectivity and stability of CL biosensor

The selectivity of the 3D μPAD based CL biosensor was further evaluated. Four different kinds of specific oxidase was immobilized on the four detection zones for the determination of glucose, lactate, cholesterol, and choline, respectively. The selectivity was evaluated by comparing the CL intensities generated from the four detection zones incubated with blank, 0.5 mmol/L glucose, 2.0 mmol/L lactate, 0.2 mmol/L cholesterol, 0.5 mmol/L choline, and mixture of the four analytes. The obtained CL intensities were shown in Fig. 4. As expected, the target analyte of the detection zone and the mixture containing the target analyte exhibited similar high CL intensities. In comparison, the CL intensities from the blank and the non-target analytes were rather weak. Thus, the μPAD based CL biosensor in this work exhibited high selectivity for the detection of glucose, lactate, cholesterol, and choline. Such high selectivity was mainly attributed to the high specificity of the enzymatic reactions.

The stability of the developed μPAD was also examined. The fabricated μPADs were stored in dry sealed condition at 4 °C. No remarkable change in CL responses was observed after a storage period of 30 days. The results confirmed that the device can be maintained at 4 °C for at least one month. Thus, the stability of the μPAD is acceptable.

3.6. Application in serum samples

The practical application ability of the proposed 3D μPAD was investigated by the simultaneous determination of glucose, lactate,

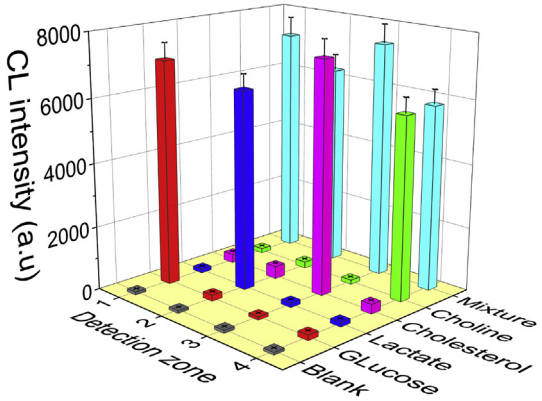

Fig. 4. CL responses for different analytes at four detection zones. Detection zone No.1: glucose detection zone, No.2: lactate detection zone, No.3: cholesterol detection zone, No.4: choline detection zone. The analytes were blank, 0.5 mmol/L glucose, 2.0 mmol/L lactate, 0.2 mmol/L cholesterol, 0.5 mmol/L choline, and mixture of 0.5 mmol/L glucose, 2.0 mmol/L lactate, 0.2 mmol/L cholesterol, and 0.5 mmol/L choline.

Table 1
The recovery of glucose, lactate, cholesterol, and choline in spiked human serum samples by using the proposed 3 D μPAD.

Analyte	Initially detected (mmol/L)	Added (mmol/L)	Total found (mmol/L)	Recovery (%)	RSD (n = 3, %)
Glucose	4.13	1.0	5.22	109	2.73
Lactate	0.97	1.0	1.91	94	2.46
Cholesterol	0.23	0.2	0.44	105	3.13
Choline	0.05	0.2	0.24	95	3.29

cholesterol, and choline in human serum samples. The normal concentrations of glucose, lactate, cholesterol, and choline in human serum sample are 2.5–5.3 mmol/L (Tietz, 1990), 0.5–1.7 mmol/L (Tietz, 1990), 2.86–5.98 mmol/L (Tietz, 1990), and around 10 μmol/L (Ulus et al., 1998), respectively. Particularly, the low detection limits of this 3D μPAD enabled the detection of glucose, lactate, cholesterol, and choline in diluted samples. Thus, only microliter grade serum samples were needed. The serum samples were diluted properly by phosphate buffer (pH 7.0) prior to the measurements. The detection results are shown in Table 1. The determined concentrations of glucose, lactate, cholesterol, and choline in the samples were in the normal concentration ranges, which are in good agreements with the reported values. The accuracy of the proposed 3D μPAD based CL biosensor was further evaluated by recovery experiments. The serum sample was further spiked with 1 mmol/L glucose, 1.0 mmol/L lactate, 0.2 mmol/L cholesterol, and 0.2 mmol/L choline. The recoveries of spiked glucose, lactate, cholesterol, and choline in the serum sample ranged from 94% to 109%. And the RSD for three repeated measurements were below 3.29%. The satisfactory recoveries and RSD indicated that the proposed μPAD based CL biosensor has good accuracy and is applicable for multiplexed quantitative analysis of glucose, lactate, cholesterol, and choline in biological samples for POCT diagnosis.

4. Conclusion

In this work, a simple 3D μPAD with high resolution temporally resolved CL emissions has been developed through double-layered 3D branched microfluidic channel design for the first time. The obtained temporally resolved CL peaks were steep, stable and base-line separated with resolutions as high as 21.2–24.3 (much higher than 1.5). Improved resolution, reproducibility and sensitivity were obtained by virtue of the double-layered 3D μPAD design rather than traditional one-layered 2D μPAD design. The temporally resolved CL emission peaks obtained at different times in the CL kinetic curve could be used for multiplexed CL analysis. Then, a multiplexed CL biosensor has been developed for the sensitive, selective and simultaneous determination of glucose, lactate, cholesterol, and choline in serum samples based on the fabricated 3D μPAD. To the best of our knowledge, this work shows the first example of μPAD based CL biosensor for the simultaneous determination of glucose, lactate, cholesterol and choline with high sensitivity. Furthermore, tunable numbers such as three, four, five, etc. temporally resolved CL emission peaks could be obtained by rationally designing the pattern of the μPAD. Moreover, the proposed 3D μPAD based CL sensing strategy can be readily expanded to multiplexed determination of other small biomolecules such as uric acid, cortisol, and bilirubin by using their specific H_2O_2-producing oxidases. The proposed 3D μPAD might also be adapted to the multiplexed determination of other biomarkers involved with other CL reaction systems, and even be combined with portable and widespread smartphone as detector. And recently we have successfully captured the spatially and temporally resolved CL images by using the proposed 3D μPAD as sensing platform and smartphone as detector. More detailed research are under investigations. This work provides a new strategy for the fabrication of simple 3D μPAD with high resolution temporally resolved CL emissions for multiplexed CL analysis, which holds great application potential for point-of-care diagnosis.

Conflict of interests

The authors declare that there is no conflict of interests regarding the publication of this paper.

Declaration of interests

The authors declare that they have no known competing financial interests or personal relationships that could have appeared to influence the work reported in this paper.

The authors declare the following financial interests/personal relationships which may be considered as potential competing interests:

CRediT authorship contribution statement

Fang Li: Conceptualization, Methodology, Formal analysis, Funding acquisition, Writing - original draft, Writing - review & editing. **Jiachang Liu:** Data curation, Formal analysis. **Lei Guo:** Data curation. **Jihang Wang:** Formal analysis. **Kaiqi Zhang:** Formal analysis. **Jianbo He:** Project administration, Supervision. **Hua Cui:** Writing - review & editing, Supervision.

Acknowledgements

This work was supported by the National Natural Science Foundation of China (Grant Nos. 21605032), the Fundamental Research Funds for the Central Universities, China (Grant Nos. JZ2019HGTB0057), the State Key Laboratory of Analytical Chemistry for Life Science, Nanjing University (Grant Nos. SKLACLS1903) and the open project of Anhui province key laboratory of advanced catalytic materials and reaction engineering (Grant No. 45000-411104/007).

Appendix A. Supplementary data

Supplementary data to this article can be found online at https://doi.org/10.1016/j.bios.2019.111472.

References

Chaiyo, S., Apiluk, A., Siangproh, W., Chailapakul, O., 2016. Sensor. Actuat. B-Chem. l 233, 540–549.
Chu, W., Chen, Y., Liu, W., Zhao, M., Li, H., 2017. Sensor. Actuator. B Chem. 250, 324–332.
Ding, X., Mauk, M.G., Yin, K., Kadimisetty, K., Liu, C., 2019. Anal. Chem. 91 (1), 655–672.
Dungchai, W., Chailapakul, O., Henry, C.S., 2009. Anal. Chem. 81 (14), 5821–5826.
Gabriel, E.F., Garcia, P.T., Cardoso, T.M., Lopes, F.M., Martins, F.T., Coltro, W.K., 2016. Analyst 141 (15), 4749–4756.
Ge, L., Wang, S., Song, X., Ge, S., Yu, J., 2012. Lab Chip 12 (17), 3150–3158.
Guibal, Eric, 2004. Separ. Purif. Technol. 38 (1), 43–74.
Jang, I., Song, S., 2015. Lab Chip 15 (16), 3405–3412.
Lewis, G.G., DiTucci, M.J., Baker, M.S., Phillips, S.T., 2012. Lab Chip 12 (15), 2630–2633.
Liang, L., Lan, F., Yin, X., Ge, S., Yu, J., Yan, M., 2017. Biosens. Bioelectron. 95, 181–188.
Liang, L., Su, M., Li, L., Lan, F., Yang, G., Ge, S., Yu, J., Song, X., 2016. Sensor. Actuator. B Chem. 229, 347–354.
Lin, J.M., Shan, X., Hanaoka, S., Yamada, M., 2001. Anal. Chem. 73 (21), 5043–5051.
Lopez-Ruiz, N., Curto, V.F., Erenas, M.M., Benito-Lopez, F., Diamond, D., Palma, A.J., Capitan-Vallvey, L.F., 2014. Anal. Chem. 86 (19), 9554–9562.
Martinez, A.W., Phillips, S.T., Butte, M.J., Whitesides, G.M., 2007. Angew. Chem. Int. Ed. 46 (8), 1318–1320.
Mike, J.H., Cleland, T.J., 1992. Anal. Chim. Acta 259 (1), 73–78.
Morbioli, G.G., Mazzu-Nascimento, T., Milan, L.A., Stockton, A.M., Carrilho, E., 2017a. Anal. Chem. 89 (9), 4786–4792.
Morbioli, G.G., Mazzu-Nascimento, T., Stockton, A.M., Carrilho, E., 2017b. Anal. Chim. Acta 970, 1–22.
Nakamura, H., Murakami, Y., Yokoyama, K., Tamiya, E., Karube, I., Suda, M., Uchiyama, S., 2001. Anal. Chem. 73 (2), 373–378.
Rattanarat, P., Dungchai, W., Cate, D., Volckens, J., Chailapakul, O., Henry, C.S., 2014. Anal. Chem. 86 (7), 3555–3562.
Rinaudo, M., 2006. Prog. Polym. Sci. 31 (7), 603–632.

Syedmoradi, L., Daneshpour, M., Alvandipour, M., Gomez, F.A., Hajghassem, H., Omidfar, K., 2017. Biosens Bioelectron 87, 373–387.
Tietz, N.W., 1990. Clinical Guide to Laboratory Test, second ed. W.B.
Tsafack, V.C., Marquette, C.A., Pizzolato, F., Blum, J., c, L., 2000. Biosens. Bioelectron. 15 (3), 125–133.
Ulus, I.H., Özyurt, G., Korfali, E., 1998. Neurochem. Res. 23 (5), 727–732.
Wang, S., Ge, L., Song, X., Yu, J., Ge, S., Huang, J., Zeng, F., 2012. Biosens. Bioelectron. 31 (1), 212–218.
Wang, X., Li, F., Cai, Z., Liu, K., Li, J., Zhang, B., He, J., 2018. Anal. Bioanal. Chem. 410 (10), 2647–2655.
Xia, Y., Si, J., Li, Z., 2016. Biosens. Bioelectron. 77, 774–789.
Yamada, K., Henares, T.G., Suzuki, K., Citterio, D., 2015. Angew. Chem. Int. Ed. 54 (18), 5294–5310.
Yu, J., Ge, L., Huang, J., Wang, S., Ge, S., 2011. Lab Chip 11 (7), 1286–1291.